

Simulated Performance Analysis of a Composite Vector Tracking and Navigation Filter

Christopher R. Hamm and David M. Bevly
Auburn University, Auburn, Alabama

BIOGRAPHY

Christopher R. Hamm is an M.S. candidate in the Department of Electrical and Computer Engineering at Auburn University where he received a B.S in Computer Engineering in 2003. He is currently working as a research assistant in the GPS and Vehicle Dynamics Lab (GaVLab) in the Department of Mechanical Engineering at Auburn University. His area of research involves performance comparisons of GPS/INS coupling techniques for use in high noise/high dynamic environments.

David M. Bevly received his B.S. from Texas A&M University in 1995, M.S from Massachusetts Institute of Technology in 1997, and Ph.D. from Stanford University in 2001 in Mechanical Engineering. He joined the faculty of the Department of Mechanical Engineering at Auburn University in 2001 as an assistant professor. Dr. Bevly is the director of Auburn University's GPS and Vehicle Dynamics Laboratory which focuses on the control and navigation of vehicles using GPS in conjunction with other sensors, such as Inertial Navigation System (INS) sensors.

ABSTRACT

This paper presents an alternative GPS signal tracking method which uses an extended Kalman-Bucy filter in place of traditional independent, parallel tracking loops. Furthermore, this method is extended into a combined tracking and navigation filter coupled with inertial aiding. This approach reduces filter design complexity significantly and allows for optimal navigation performance in a variety of conditions. Specifically, the proposed method is demonstrated under high dynamics while experiencing significant levels of jamming. A simulation in a single-axis configuration was used to compare the proposed method to an existing aided fixed-gain method to ascertain the expected level of anti-jam performance as well as immunity to dynamic stress. Results from this simulation indicate

a nominal expected positioning performance improvement of 5 meters with improvements of up to 25 meters in some cases. A simulation comparing IMU's of differing grades was also run to ascertain the proposed method's dependence upon inertial sensor quality.

INTRODUCTION

Today, the heavy reliance on GPS as a ubiquitous navigation system has made GPS a mission-critical system even in the civilian sector. Unfortunately, the relatively low received signal power makes satellite signal reception vulnerable to radio frequency interference whether that interference is intentional or unintentional. Using traditional fixed-gain tracking loops, this vulnerability may be decreased by reducing the closed-loop bandwidth of the tracking loops which has the effect of decreasing the received noise power. This decrease in tracking loop bandwidth introduces a new issue – stress from platform dynamics [1]. The dynamics of the receiver platform induces a stress in the tracking of the received signal via a Doppler shift. To track this Doppler shift, the tracking loop typically must have a wider bandwidth. Obviously this presents a crux to GPS receiver design.

One approach to reduce or possibly remove the dynamic stress in the signal tracking loops is to provide inertial aiding. Using a six degree of freedom inertial measurement unit (6DOF IMU), a line-of-sight acceleration estimate can be computed and integrated to obtain a line-of-sight velocity. Converting this velocity into the proper units and adding into the tracking loop computations allows the tracking loop to maintain tracking at a lower closed-loop bandwidth under high dynamics experienced at the receiver. This approach is an improvement but still relies on a fixed-bandwidth filter to track the received signal. Since RFI levels will most likely vary over time and location, an adaptive-gain filter would offer superior performance under a wider variety of conditions. This paper seeks to present just such a method. The method pre-

sented here combines inertial measurements with discriminator outputs in a Kalman filter arrangement to produce an adaptive tracking framework that is nearly immune to dynamic stress effects even in areas where the received noise power is rather high. This method is further extended to provide a navigation solution as well similar to [2] and [3].

TRADITIONAL TRACKING LOOPS

The basic architecture of a signal tracking loop is shown in Figure 1. In general, a tracking loop consists of three major components: a comparator or discriminator, a filter, and an oscillator. A comparator functions like its namesake; the received signal and estimated signal are compared and a measure of error between the two is produced. In some tracking loops, a simple scalar comparison is not possible or practical. Instead, several combinations of the estimated signal and the received signal are produced. A discriminator operates on these multiple combinations to produce a single measure of error. The typical loop filter is a low-pass filter with one or more integral terms. Integral terms in the loop filter determine the kinds of dynamics in the received signal that a loop can track. The third component of a tracking loop is the numerically-controlled oscillator whose frequency is controlled by the output of the loop filter.

Two of the types of tracking loops common to most GPS receivers are delay-locked loops (DLL's) and phase-locked loops (PLL's). In the descriptions that follow, the received signal is assumed to be

$$r(t, \mathbf{x}) = p(t, \mathbf{x}) \sin(\theta(t, \mathbf{x})) + n(t) \quad (1)$$

having two components to be tracked: the code signal, $p(t, \mathbf{x})$ and the carrier signal, $s(t, \mathbf{x})$ which is equivalent to $\sin(\theta(t, \mathbf{x}))$. Most GPS receivers use a phase-locked loop to track the carrier component of a received signal. While some formulations of a PLL are capable of tracking a BPSK signal like the one transmitted by GPS satellites, a more typical approach is to use a Costas loop, which is a subtype of phase-locked loops. Under a Costas arrangement, the received signal is split into two branches with one branch being combined with an *in-phase* estimate of the received carrier component and the other branch being combined with a *quadrature-phase* (i.e., 90 degrees out of

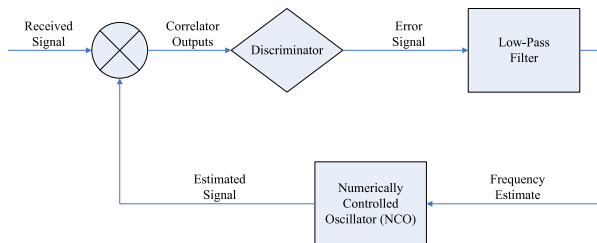


Fig. 1 Basic Tracking Loop Architecture

phase with the in-phase branch) estimate of the received carrier component. These branches are often referred to as I and Q channels respective to their signal components. At each iteration of the loop, the Costas loop discriminator uses the I and Q measurements to generate a measure of the phase error between the received signal and the replica signal. While several common discriminator functions exist, the most powerful as well as the most computationally intensive function is an arctangent discriminator shown in (4) while the output of this discriminator function is shown in Figure 2.

$$I = r(t, \mathbf{x})p(t, \hat{\mathbf{x}}) \sin(\theta(t, \hat{\mathbf{x}})) \quad (2)$$

$$Q = r(t, \mathbf{x})p(t, \hat{\mathbf{x}}) \cos(\theta(t, \hat{\mathbf{x}})) \quad (3)$$

$$D(\epsilon_s) = \arctan\left(\frac{Q}{I}\right) \quad (4)$$

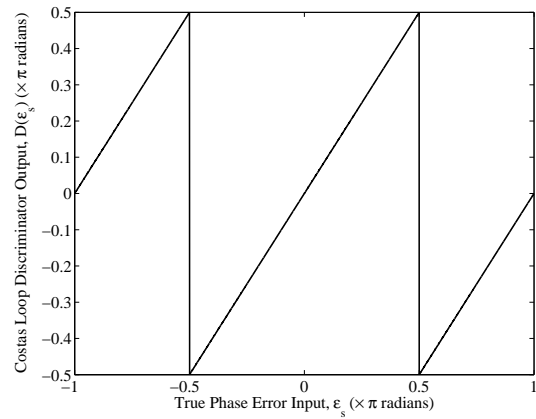


Fig. 2 Carrier Loop Discriminator Curve

After the discriminator, signal flow through a Costas loop continues as in a basic tracking loop with the signal separating back into the I and Q channels after the oscillator as shown in Figure 3.

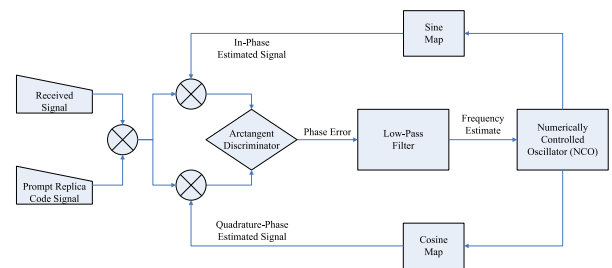


Fig. 3 Carrier Tracking Loop

Delay-locked loops, as utilized in GPS receivers, track the PRN code sequence. After the initial acquisition phase in which the code generator is initialized to the proper chip offset, the code generator splits the incoming I and Q channels into three more channels each for a total of six channels in all. One of three replica code signals are applied

to each I and Q channel to make up the six new channels or *correlators*. The three replica code sequences are the prompt, early, and late sequences. The prompt sequence is the aligned estimate of the received code sequence. The early and late sequences are shifted versions of the prompt sequence where the early sequence is a half-chip advance and the late sequence is a half-chip delay. Other chip spacings are possible (up to a maximum of one full-chip), but one half-chip is the most common correlator spacing used. The correlator outputs from the code generator are described by (5 - 10). The most accurate discriminator used in delay-locked loops is the dot product discriminator which is described in (11) and whose output is illustrated in Figure 4.

$$I_E = r(t, \mathbf{x})p(t + \tau, \hat{\mathbf{x}}) \sin(\theta(t, \hat{\mathbf{x}})) \quad (5)$$

$$Q_E = r(t, \mathbf{x})p(t + \tau, \hat{\mathbf{x}}) \cos(\theta(t, \hat{\mathbf{x}})) \quad (6)$$

$$I_P = r(t, \mathbf{x})p(t, \hat{\mathbf{x}}) \sin(\theta(t, \hat{\mathbf{x}})) \quad (7)$$

$$Q_P = r(t, \mathbf{x})p(t, \hat{\mathbf{x}}) \cos(\theta(t, \hat{\mathbf{x}})) \quad (8)$$

$$I_L = r(t, \mathbf{x})p(t - \tau, \hat{\mathbf{x}}) \sin(\theta(t, \hat{\mathbf{x}})) \quad (9)$$

$$Q_L = r(t, \mathbf{x})p(t - \tau, \hat{\mathbf{x}}) \cos(\theta(t, \hat{\mathbf{x}})) \quad (10)$$

$$D(\epsilon_p) = \frac{(I_E - I_L)I_P + (Q_E - Q_L)Q_P}{\sqrt{I_P^2 + Q_P^2}} \quad (11)$$

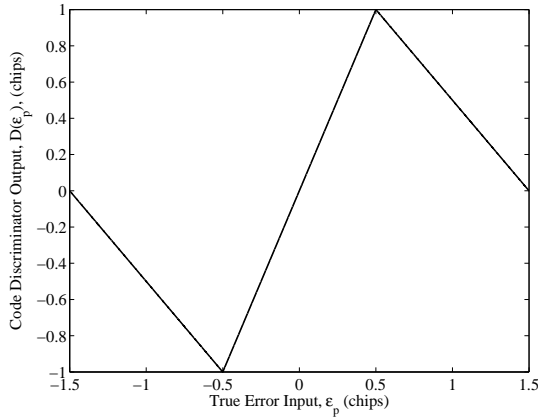


Fig. 4 Code Loop Discriminator Curve

GPS AND KALMAN FILTERING

A Kalman filter is an optimal, recursive state estimation technique which under the proper assumptions provides the optimal estimate of system state with regard to both system disturbances and noise in the measured signal. Furthermore, if the assumed values are incorrect but near the correct values, the performance of the Kalman filter is near optimal. The role of Kalman filtering in GPS is extensive and well documented through out the literature and a thor-

ough treatment of Kalman filtering and estimation is given in [4, 5, 6] with particular attention given to GPS in [6]

While there are regularly used techniques for approximating nonlinear systems by linear models, some systems exhibit dynamics which do not permit such approximations from being practically used. GPS navigation is one such system whose dynamic behavior does not lend itself to a linear Kalman filter approach. One nonlinear estimation technique is the extended Kalman filter whose algorithm is altered to use a nonlinear estimation of measurement and a nonlinear propagation of state using standard techniques for solving ODE initial-value problems, such as Runge-Kutta. Equations (13) and (14) show the relevant changes to state update and the state propagation where $g(t, \hat{\mathbf{x}})$ is the nonlinear measurement function and $f(t, \hat{\mathbf{x}}, \mathbf{u})$ is the nonlinear state equation. An additional requirement for this algorithm is that the Jacobians of the measurement functions, C , and the state functions, A , must be updated at each iteration. Also, the Jacobian of the state function, A , must also be discretized at every iteration.

$$\hat{\mathbf{x}}_k^{(+)} = \hat{\mathbf{x}}_k^{(-)} + L_k (\mathbf{y}_k - \hat{\mathbf{y}}_k) \quad (12)$$

$$= \hat{\mathbf{x}}_k^{(-)} + L_k \left(\mathbf{y}_k - g \left(\hat{\mathbf{x}}_k^{(-)} \right) \right) \quad (13)$$

$$\hat{\mathbf{x}}_{k+1}^{(+)} = \hat{\mathbf{x}}_k^{(+)} + \int_k^{k+1} f(t, \hat{\mathbf{x}}, \mathbf{u}) d\tau \quad (14)$$

While this approach is appealing and useful in many applications, the extended Kalman filter suffers from a numerically undesirable necessity. While the propagation of state is computed using standard ordinary differential equation integration routines, a discrete-time, linear matrix is still required for the propagation of the estimate error covariance estimate, P_k . To compute this matrix requires the computation of a matrix exponential which is expensive to calculate numerically, particularly if it is done at every time step. A simple alternative is the extended Kalman-Bucy filter [5] which replaces the discrete propagation of the esti-

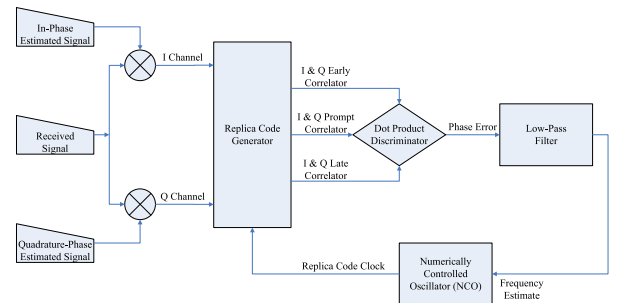


Fig. 5 Code Tracking Loop

mate error covariance estimate with (15).

$$P_{k+1}^{(-)} = P_k^{(+)} + \int_k^{k+1} [AP_k^{(+)} + P_k^{(+)}A^T + Q'] d\tau \quad (15)$$

$$Q' = B_w Q_c B_w^T \quad (16)$$

INERTIAL SENSOR ERROR MODELS

Inertial sensors such as accelerometers and gyroscopes provide a method for detecting and measuring motion in the body frame of the sensing platform. Inertial sensors benefit from a relative immunity to most radio frequency interference (RFI) experienced in GPS reception. Using coordinate transformations and integration techniques, position, velocity, and attitude of the platform in a global frame can be determined from the obtained inertial sensor measurements. From this point, techniques for combing these inertial navigation solutions with GPS signals are numerous and varied [7]. To successfully augment the GPS navigation solution with inertial sensors, error sources in the inertial measurements must be examined and compensation for their effects must be made. While many kinds of error sources are present in inertial sensors, three prominent ones, which are examined in this paper, are random walk, w ; bias, b ; and scale factor, SF . A simple model to describe these errors and their effect on the desired measurement is given in (17 - 19).

$$u(t) = SF(\alpha(t)) + b(t) + w_u(t) \quad (17)$$

$$\dot{b}(t) = \frac{-1}{\tau_b} + w_b(t) \quad (18)$$

$$\dot{SF}(t) = 0 \quad (19)$$

where

- $u \equiv$ Sensor Measurement
- $\alpha \equiv$ True Dynamic Quantity
(e.g., Acceleration or Rotation Rate)
- $b \equiv$ Bias
- $SF \equiv$ Scale Factor
- $w \equiv$ Gaussian Noise

The Kalman filter discussed previously provides an excellent mechanism for mitigating the effects of errors in inertial measurements when combined with an external measurement such as GPS and is an approach examined later in this paper.

INTEGRATED VECTOR TRACKING LOOPS

In a GPS receiver, the most fundamental type of measurement is the correlator outputs with each receiver having at least four correlators per channel. Each correlator

is a nonlinear combination of the received signal and the receiver's estimate of the signal. Typically, these measurements are combined according to as discriminator function to produce a linear or nearly linear estimate of the error between the received signal and the estimated signal. The algorithm under investigation here takes as its primary measurement these correlator outputs rather than using an intermediary computation such as pseudorange.

Tracking Loops as Kalman filters

Phase-locked loops and delay-locked loops are a form of nonlinear output estimator but do not lend themselves to the use of an extended Kalman-Bucy filter to handle the nonlinearities. The primary nonlinear components in a PLL or DLL are the discriminator and the NCO. The extended Kalman-Bucy filter still relies on a linear computation of the error between the received signal and estimated signal. While PLL's and DLL's are typically modeled as linear systems based on a small phase angle approximation, these tracking loops may be modeled as linear systems over a much wider range without loss of accuracy under two conditions: (1) the loop discriminator uses a function whose output is linear, and (2) the NCO output appears to be a linear integration to low-pass filter. In the case of the carrier tracking loop, the arctangent function used in a Costas-loop arrangement provides linear output as shown in Figure 2. While the output is only linear between $\pm \frac{\pi}{2}$ radians, this range is both typical and more than adequate for Costas PLL tracking. Similarly in the case of the code tracking loop, a normalized dot product function provides the linear output shown in Figure 4 with the linear range of $\pm \frac{1}{2}$ chips. With regard to the linearity of the NCO, the input to the NCO must be linear in output as perceived at the output of the discriminator. The resultant linear model of the tracking loop diagram shown in Figure 1 is shown in Figure 6. For the purpose of an example continued throughout this paper, a second-order loop is shown in the diagram and its closed-loop transfer function from received signal, $Y(s)$ to estimated signal, $\hat{Y}(s)$, is given in (20).

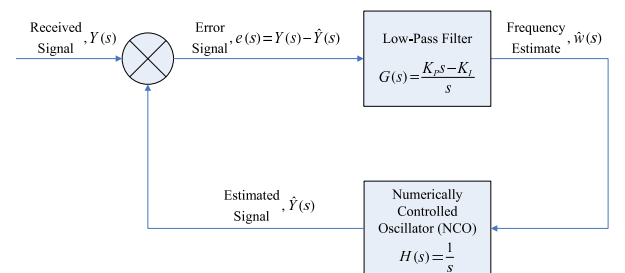


Fig. 6 Linear Model of a Basic Tracking Loop

$$\frac{\hat{Y}(s)}{Y(s)} = \frac{K_{PS} - K_I}{s^2 + K_{PS} - K_I} \quad (20)$$

A linear model in transfer function form implies that a state-variable representation can be formed assuming that the system is completely observable. Beginning with the following substitutions,

$$\begin{aligned}\hat{X}_1(s) &= \hat{Y}(s) \\ U(s) &= Y(s)\end{aligned}$$

$$s^2 \hat{X}_1(s) + K_P s \hat{X}_1(s) - K_I \hat{X}_1(s) = K_P s U(s) - K_I U(s) \quad (21)$$

$$s^2 \hat{X}_1(s) = -K_P s \hat{X}_1(s) + K_P s U(s) + K_I \hat{X}_1(s) - K_I U(s) \quad (22)$$

$$s \hat{X}_1(s) = -K_P \hat{X}_1(s) + K_P U(s) + \frac{K_I}{s} \hat{X}_1(s) - \frac{K_I}{s} U(s) \quad (23)$$

$$\hat{X}_2(s) = \frac{K_I}{s} \hat{X}_1(s) - \frac{K_I}{s} U(s) \quad (24)$$

$$s \hat{X}_1(s) = -K_P \hat{X}_1(s) + K_P U(s) + \hat{X}_2(s) \quad (25)$$

$$s \hat{X}_2(s) = K_I \hat{X}_1(s) - K_I U(s) \quad (26)$$

$$s \hat{\mathbf{X}}(s) = \begin{bmatrix} -K_P & 1 \\ K_I & 0 \end{bmatrix} \hat{\mathbf{X}}(s) + \begin{bmatrix} K_P \\ -K_I \end{bmatrix} \mathbf{U}(s) \quad (27)$$

$$\dot{\hat{\mathbf{x}}}(t) = \mathcal{L}^{-1} \left\{ s \hat{\mathbf{X}}(s) \right\} \quad (28)$$

$$\dot{\hat{\mathbf{x}}}(t) = \begin{bmatrix} -K_P & 1 \\ K_I & 0 \end{bmatrix} \hat{\mathbf{x}}(t) + \begin{bmatrix} K_P \\ -K_I \end{bmatrix} \mathbf{u}(t) \quad (29)$$

The estimator dynamics for a classical, fixed-gain estimator can be described as

$$\dot{\hat{\mathbf{x}}}(t) = (A - LC) \hat{\mathbf{x}}(t) + L\mathbf{y}(t) \quad (30)$$

Thus, the analogous relationship between signal tracking loops and state estimation filters becomes apparent by comparing (29) to (30). The extension from a classical estimator to a Kalman estimator is a matter of computing the estimation gain, L , recursively based on the known characteristics of the system's disturbances and sensor noise.

Implementing this analogue requires a formulation of state equations which relate correlator measurements to code or carrier phase. A generic set of state equations to describe the phase and frequency of a code or carrier signal is shown in (31 - 33).

$$\mathbf{x} = \begin{bmatrix} \theta \\ \omega \end{bmatrix} = \begin{bmatrix} \text{Phase} \\ \text{Frequency} \end{bmatrix} \quad (31)$$

$$\dot{\mathbf{x}} = \begin{bmatrix} \omega \\ w \end{bmatrix} \quad (32)$$

$$\mathbf{y} = [\theta + v] \quad (33)$$

In traditional GPS tracking loops, the phase measurements themselves are not available or occur at such a high sample rate as to make them unusable. Instead, a non-linear discriminator function forms an error estimate using the correlator measurements. This error estimate becomes the innovation term of a classical estimator so that the estimator dynamics for the general case become

$$\dot{\hat{\mathbf{x}}}(t) = A\hat{\mathbf{x}}(t) + LD(\epsilon(t))$$

So far, the formulation of the tracking loops as classical state estimators has been given as continuous time state equations. However, the correlators, and subsequently, the discriminator and tracking loops update at discrete intervals based on the pre-detection integration time. Thus, the state estimators, which are replacing the tracking loops, must also update at the same discrete interval.

The propagation of the estimate error covariance matrix over time relies on the process noise covariance matrix, $Q = E[w^T w]$, and the measurement noise covariance matrix, $R = E[v^T v]$. Subsequently, the computation of the estimator gains depend on these two matrices as well. The measurement noise covariance is composed of two terms, the noise due to the environment (e.g., thermal noise, RF interference, intentional jamming) and the receiver's oscillator noise. The environmental noise covariance can be approximated by $\frac{2}{C/N_o T}$ where T is the pre-detection integration interval. Using the current formulation of the state equations, analytically derived values for the process noise covariance which relate to the system physically may not be available. Instead, an estimate of the process noise covariance should be formed based on some expectation of the receiver's dynamics. The process noise should be modeled as entering the system at the highest model dynamic. In the formulation given, this dynamic is frequency and as such the unknown or untracked dynamic effect would be acceleration and an appropriate approximation of the process noise might be

$$\sigma_w^2 = \frac{1}{N} \sum_{k=0}^N \left(\frac{a_k}{\lambda} \right)^2 - \left(\frac{1}{N} \sum_{k=0}^N \frac{a_k}{\lambda} \right)^2 \quad (34)$$

where a_k is the line-of-sight acceleration at a sample interval, N is some arbitrarily chosen number of samples, and λ is the wavelength of the signal being tracked. Since the bandwidth of a Kalman estimator from measurement to estimate is based on the ratio between the measurement and process noise covariance matrices, modeling the process noise by this method is similar to designing fixed-gain tracking loops using the design constraints of carrier-to-noise ratios and desired dynamic stress performance.

Inertial Augmentation

Traditional GPS signal tracking fails under high-dynamics experienced by the receiver platform. The same

is also true for the vectorized tracking loop shown above as it also lacks a measurement of the experienced dynamic behavior of the receiver. The Kalman filter as shown thus far only has prior knowledge of the expected noise characteristics in the environment of operation and an approximation of the expected platform dynamics. To provide tracking and navigation under high dynamics, the governing state equations can be altered so that inertial sensors directly aid the signal tracking aspect. Using the sensor models discussed previously, accelerometer measurements are applied as inputs, \mathbf{u} , to the state equations. These measurements are assumed to be in the axis of modeled motion (i.e., satellite line-of-sight).

As discussed previously in this paper, the relevant error sources for a single axis accelerometer are scale factor, S_F , bias, $b(t)$, and random walk, w . Using the models error model given in (17 - 19), an inertially aided tracking filter which compensates for errors in the inertial sensor is given in (36 - 38). In this model, both bias and scale factor are modeled as first-order Markov processes and incorporated into the state vector to be estimated by the Kalman filter. While bias may be modeled as a zeroth-order Markov process, the first-order process more accurately simulates the observed bias behavior of an inertial sensor. In the case of scale factor, the observed scale factor is constant but modeling the scale factor term as a Markov process with a very large time constant (i.e., varying very slowly) prevents the Kalman estimate of that term from going to steady-state prior to reaching an accurate estimate of the scale factor. The covariance of the driving noise for these process models along with the random walk form the process noise covariance matrix, Q_c , and replaces the dynamic approximation given in (34).

$$\mathbf{x} = \begin{bmatrix} \theta \\ \omega \\ b \\ S_F \end{bmatrix} \quad (35)$$

$$= \begin{bmatrix} \text{Phase} \\ \text{Frequency} \\ \text{Accelerometer Bias} \\ \text{Accelerometer Scale Factor} \end{bmatrix} \quad (36)$$

$$\dot{\mathbf{x}} = \begin{bmatrix} \omega \\ \frac{gu-b}{\lambda S_F} + w_u \\ \frac{-1}{\tau_b} + w_b \\ \frac{-1}{\tau_{S_F}} + w_{S_F} \end{bmatrix} \quad (37)$$

$$\mathbf{y} = [\theta + v] \quad (38)$$

Extending the Tracking Filter to Navigation

As GPS signals are in some ways similar to a kind of radar signal, the measured and/or estimated components of a received signal are analogous to the navigational states of the receiver. Delta phase is analogous to position; delta

frequency is analogous to velocity; and change in delta frequency is analogous to acceleration. In each case, the link between the realms is a linear scaling by the signal wavelength, λ , which has units of meters per signal period. Thus,

$$P_x = \lambda(\theta_0 - \theta) = \lambda\Delta\theta \quad (39)$$

$$V_x = \lambda(\omega_0 - \omega) = \lambda\Delta\omega \quad (40)$$

$$A_x = \lambda(\dot{\omega}_0 - \dot{\omega}) = \lambda\Delta\dot{\omega} \quad (41)$$

Using this linear relation, the vector tracking filter described thus far may be extended to provide navigation solutions as well. This extension is possible only if the initial state estimate error is less than the discriminator tracking range in meters. If the extension is possible, the resulting equations become

$$\mathbf{x} = \begin{bmatrix} P_x \\ V_x \\ b \\ S_F \end{bmatrix} = \begin{bmatrix} \text{Position} \\ \text{Velocity} \\ \text{Accelerometer Bias} \\ \text{Accelerometer Scale Factor} \end{bmatrix} \quad (42)$$

$$\dot{\mathbf{x}} = \begin{bmatrix} P_x \\ \frac{gu-b}{S_F} + w_u \\ \frac{-1}{\tau_b} + w_b \\ \frac{-1}{\tau_{S_F}} + w_{S_F} \end{bmatrix} \quad (43)$$

$$\mathbf{y} = [\theta + v] = [\lambda P_x + v] \quad (44)$$

As a matter of practical implementation of this method several issues must be addressed. The search range required to perform an acquisition and hand-off to navigation is prohibitively large. As such, standard receiver algorithms must be used to initialize the tracking/navigation filter estimate of position and velocity. Secondly, the total positioning error in the initial estimate must be less than half the wavelength of the signal being tracked. For code tracking, this positioning requirement is 146.53 meters while for carrier tracking the estimate error must be less than 9.515 centimeters. The requirements on the velocity estimate are slightly more abstract. In each case the velocity estimate error multiplied by the filter update rate must not exceed the tracking requirements imposed by the position state. Finally, in light of the 9.5 centimeter requirement for carrier tracking, a tracking and navigation filter for carrier signals requires the use of carrier-phase differential GPS techniques to resolve the initial position. Additionally, cycle slips in carrier tracking pose a significant issue to the usability of this method.

SIMULATION & RESULTS

To validate this vectorized approach to tracking and navigation, a single axis simulation was performed in which the

receiver begins from rest, moves directly toward the satellite, and eventually comes to rest again. The generalized acceleration profile is shown in Figure 7. The maximum jerk experienced in each run was $\gamma 10 \frac{m}{s^3}$ where γ was the coefficient of acceleration of the profile. The jamming profile exerted on the receiver mimicked the platform moving directly toward a wide-band Gaussian emitter. The profile began at a nominal J/S of 35 dB and increased linearly with position to the maximum J/S value as reported in each run. Thus, at the final position the receiver is experiencing maximum jamming power. The inertial sensor measurements used were a single accelerometer aligned with axis of motion. As such, no coordinate transformations were necessary. The inertial sensor quality simulated was equivalent to an accelerometer found in a tactical grade IMU [8]. The sampling rate of the simulated inertial sensors was 200 Hz while the pre-detection interval for the simulated GPS signals was 20 milliseconds (i.e., 50 Hz update rate). Since oscillator stability and phase noise play a large role in tracking loop performance, additional white noise was added to the received signal to approximate the effects of temperature controlled oscillator (TCXO) as given in [9]. For comparison purposes, a fixed-gain inertially-aided tracking loop was simulated with the bandwidth of this tracking loop being equivalent to the steady-state bandwidth of the corresponding Kalman filter. The results of this simulation are given in Figures 8 - 11.

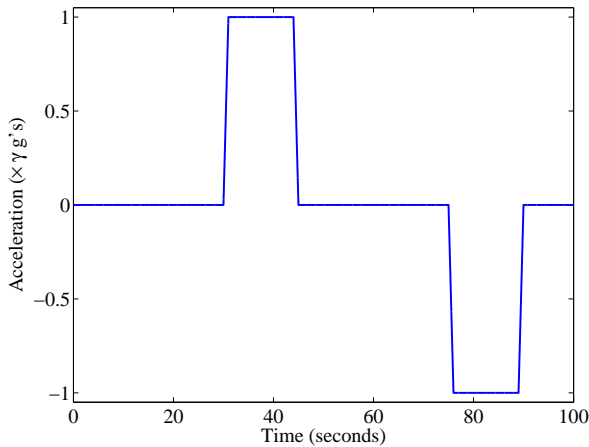


Fig. 7 Generalized Acceleration Profile

The tracking performance of both the Kalman filter approach and fixed-gain tracking loop approach are shown in Figures 8 and 9. Both approaches exhibit similar performance trends illustrating their conceptual similarities. In each case, the fixed-gain loop exhibits noticeably poorer performance than the Kalman filtering approach. As jammer power increases as shown in Figure 8, the two approaches converge in performance as both approaches rely more on the inertial aiding than the received signal power to maintain signal tracking. In Figure 9, the performance trend illustrates that the effects of dynamic stress on sig-

nal tracking have been severely diminished as judged by the even response across a wide range of dynamic accelerations.

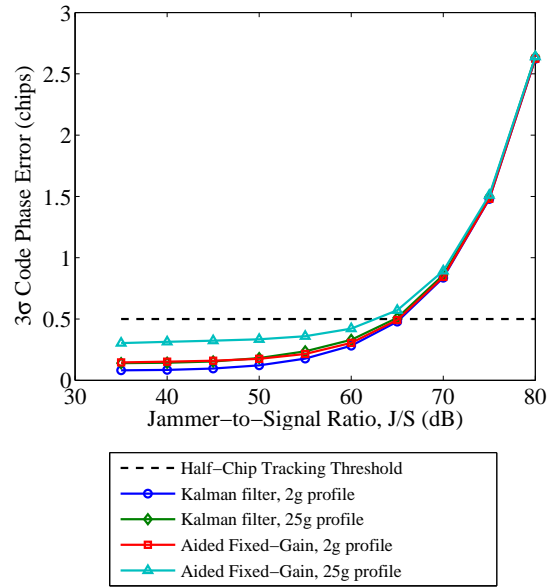


Fig. 8 Tracking Performance versus J/S

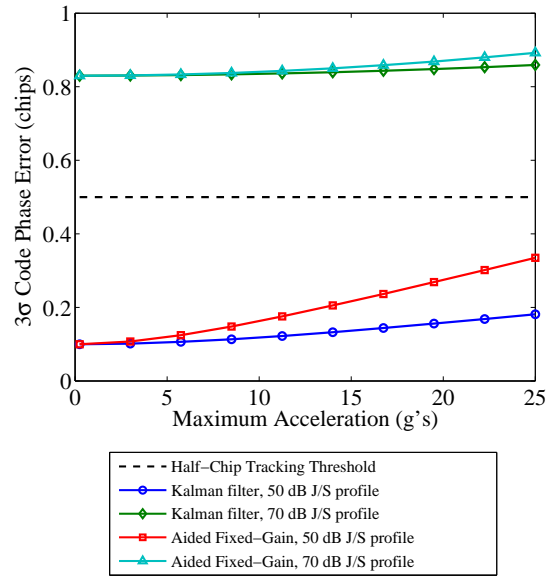


Fig. 9 Tracking Performance versus Platform Dynamics

Figures 10 and 11 demonstrate the positioning performance of the two approaches being compared. In each case, the Kalman filter approach is again superior to the fixed-gain approach. In Figure 10, a curious improvement in positioning performance occurs in both of the Kalman filter simulation profiles at the 65 dB point. One possible explanation for this performance increase is that at this

point the filter has transitioned to a reliance on the inertial inputs while GPS measurements are still of a sufficient quality to allow correction of inertial error terms. While this explanation seems to deviate from the understanding that Kalman filter gains are computed as the optimal trade-off between measurement noise and process noise, the Kalman filter gain calculation only computes gains based on the operating conditions given. If the operating conditions are suboptimal (e.g., extremely high RFI), the gains computed will also be suboptimal relative to other possible scenarios but optimal relative to the scenario in which the receiver is currently operating.

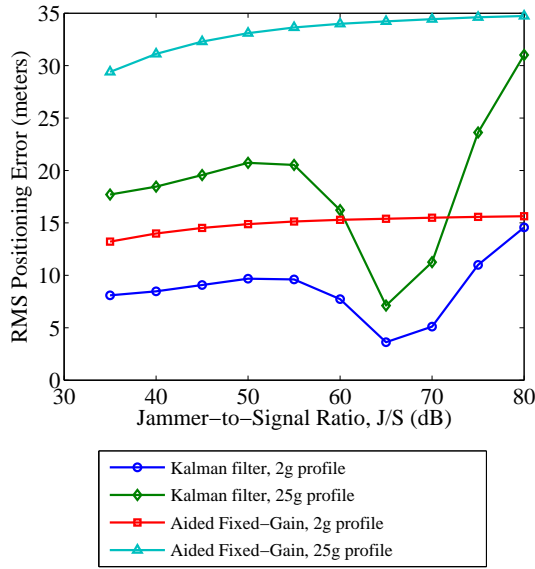


Fig. 10 Positioning Performance versus J/S

In any inertially-aided GPS scheme, the quality of inertial sensor necessary to obtain improved performance is a critical design decision. In Figures 12 - 15, simulations similar to those shown previously were run in order to compare a tactical-grade IMU versus a consumer-grade IMU typically used in general avionics and UAV applications. Table 1 provides the errors incorporated into the simulated accelerometer along with their values [8, 10]. For runs in which the jamming level was varied the maximum acceleration was held at 15 g's. For runs in which the level of dynamics was varied the maximum relative jamming power experienced was 60 dB J/S. Results for an aided fixed-gain tracking loop are excluded as the tracking loop was unable to maintain lock under the simulated scenarios.

While Figures 12 and 13 do not show a significant difference in tracking performance versus a tactical-grade IMU, the positioning performance of Kalman filter with a consumer-grade IMU is considerably worse than the demonstrated performance of the Kalman filter approach using a tactical-grade IMU. Additionally, Figure 14 shows performance with a consumer-grade IMU to be worse than

the aided fixed-gain tracking loop using a tactical-grade IMU.

Error Source	Tactical Grade	Consumer Grade
Scale Factor (% FS)	0.03	1
Bias Stability (milli-g's)	0.1	12
Velocity Random Walk (m/s/rt-hr)	19.8E-6	0.1

Table 1 Simulated Accelerometer Error Mechanisms

CONCLUSIONS

The vector tracking and navigation approach presented offers several advantages over traditional fixed-gain tracking loops as well as improvements over aided fixed-gain tracking loops. By formulating the tracking framework as a Kalman filter, augmentation of the tracking process is made considerably easier. Additionally, the complexity of designing optimal tracking loops is also reduced. While these improvements are significant, the nonlinear Kalman estimation scheme used throughout this paper also allows dynamic stress effects to be minimized while also minimizing the effects of nonlinear error terms in the inertial sensors used to aid tracking. By extending the tracking framework to further include navigation, an additional solution step is removed while not significantly adding to the overall complexity of the Kalman filter configuration. As shown in the simulation results, positioning performance is significantly improved relative to the alternative approaches presented.

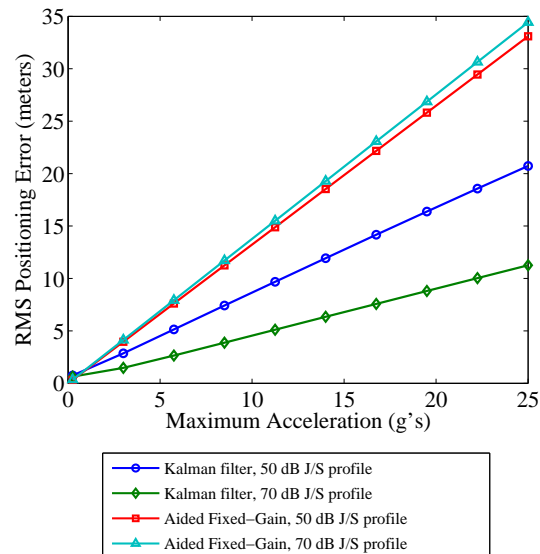


Fig. 11 Positioning Performance versus Platform Dynamics

ACKNOWLEDGMENT

This work was funded by the U.S. Army Aviation and Missile Research Development and Engineering Center (AMRDEC) at Redstone Arsenal in Huntsville, Alabama. The authors are grateful for their support.

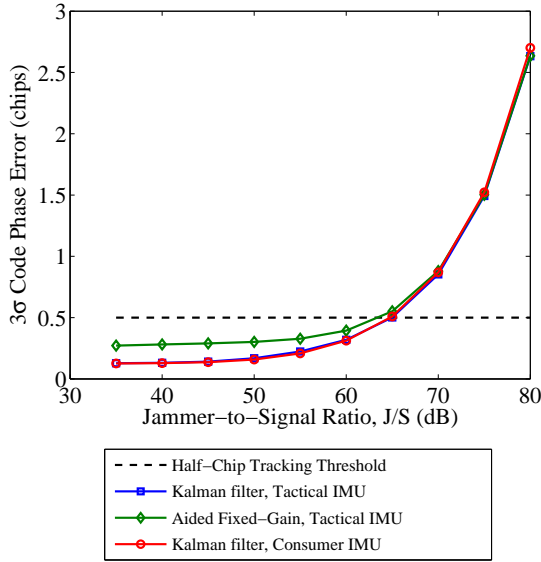


Fig. 12 Tracking Performance versus J/S (IMU Comparison)

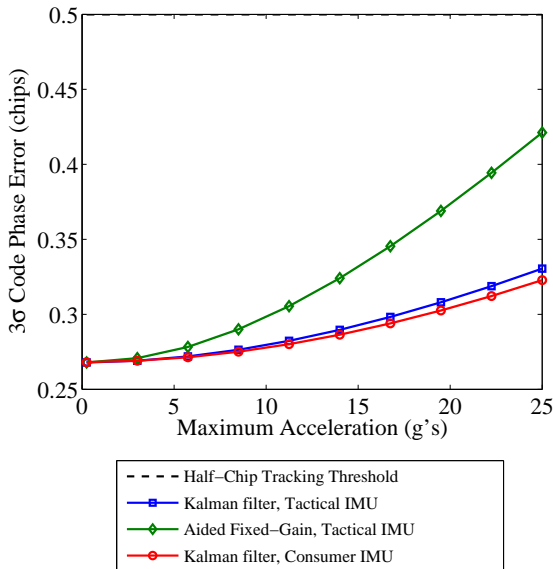


Fig. 13 Tracking Performance versus Platform Dynamics (IMU Comparison)

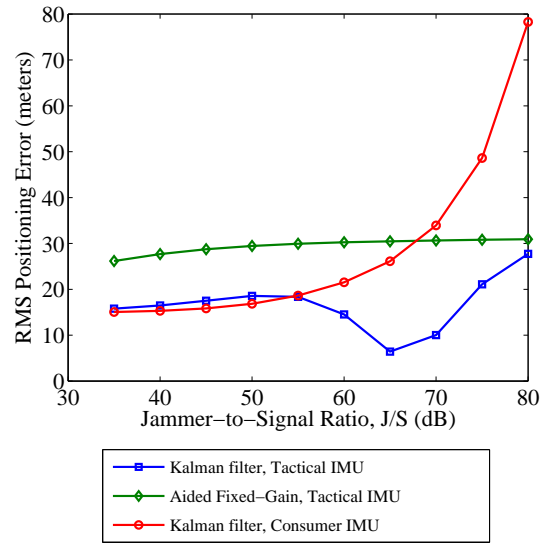


Fig. 14 Positioning Performance versus J/S (IMU Comparison)

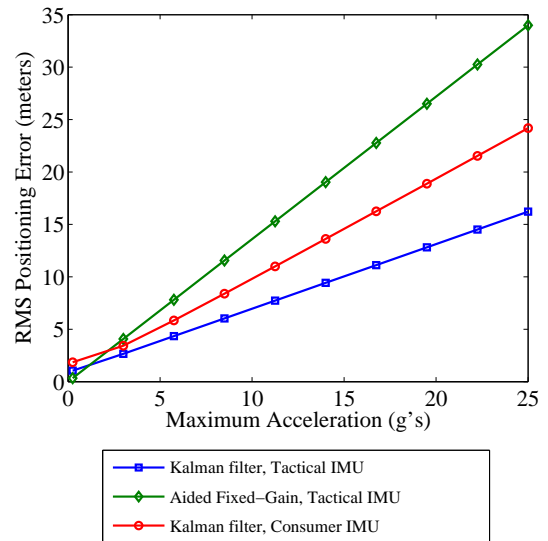


Fig. 15 Positioning Performance versus Platform Dynamics (IMU Comparison)

REFERENCES

- [1] P. Ward, "Effects of RF interference on GPS satellite signal receiver tracking," in *Understanding GPS: Principles and Applications*, ser. Mobile Communication Series, E. D. Kaplan, Ed. Artech House Publishers, 1996, ch. 6, pp. 209 – 236.
- [2] J. J. Spilker Jr., "Fundamentals of signal tracking theory," in *Global Positioning System: Theory and Applications, Volume 1*, ser. Progress in Astronautics and Aeronautics, B. W. Parkinson, Ed. Washington, DC: American Institute of Aeronautics and Astronautics, 1996, vol. 163, ch. 4.
- [3] J. M. Horslund and J. R. Hooker, "Increase jamming immunity by optimizing processing gain for GPS/INS systems," Raytheon Company, Lexington, MA, U. S. Patent 5,983160, November 1999.
- [4] A. Gelb et. al., *Applied Optimal Estimation*, A. Gelb, Ed. The M. I. T. Press, 1974.
- [5] R. F. Stengel, *Optimal Control and Estimation*. Dover Publications, 1994.
- [6] R. G. Brown and P. Y. C. Hwang, *Introduction to Random Signals and Applied Kalman Filtering*. Wiley, 1996.
- [7] R. E. Phillips and G. T. Schmidt, "GPS/INS integration," in *AGARD Lecture Series on "System Implications and Innovative Applications of Satellite Navigation"*, LS-207. Paris: NATO, July 1996, pp. 9.1–9.17.
- [8] J. G. Hanse, "Honeywell MEMS inertial technology & product status," in *Proceedings of the IEEE Position Location and Navigation Symposium, 2004*. Monterrey, CA: IEEE, April 2004, pp. 43 – 48.
- [9] D. Gebre-Egziabher et. al., "Doppler aided tracking loops for SRGPS integrity monitoring," in *Proceedings of Institute of Navigation GPS/GNSS Conference*. Portland, OR: Institute of Navigation, September 2003.
- [10] *AHRS400CD Datasheet*, Crossbow Technology, Inc., September 2005, URL: <http://www.xbow.com>.